scientific reports

Check for updates

OPEN

Wood and seagrass fibre-based materials including TPSea on hot sounding rocket structures

Raphaela Guenther[1]✉, Oliver Hohn[2], Holger Unbehaun[3], Oliver Drescher[4], Martin Tajmar[1,5], Christian Bach[1] & Hendrik Weihs[6]

In order to assess the applicability of wood- and seagrass-based materials as thermal protection system materials in space, a test with fin leading edges made of two solid woods (oak and mahogany) in the arc-heated wind tunnel L2K was conducted. The requirement analysis enabled the selection of three untreated, native solid woods (birch, oak and larch), and four wood-fibre materials (TPSea-0, -1, -C and I-WBM) for further tests. The materials from the TPSea family are developments of TUD. A more detailed screening of the materials was conducted, encompassing density, thermal conductivity, specific heat capacity, and thermogravimetric analysis. The evaluation of measurements under flight-relevant thermal loads in L2K is conducted through analysis of mass, cross-sectional area, and contour. The findings indicate that untreated solid woods are not a favoured natural material for fin leading edges, owing to substantial mass loss and uneven leading edge geometry degradation. It is evident that wood-fibre materials characterised by enhanced homogeneity, in conjunction with the incorporation of flame retardants and elevated mineral content, exhibit considerable promise with regard to optimisation. Under the single thermal load case and limited replication tested in this screening study, TPSea-C showed the most promising dimensional stability and thermal behaviour among the candidates evaluated. However, none of the investigated bio-based material variants fully meets the defined requirements. Further analyses of TPSea-C could help identify the underlying material-related limitations and provide a basis for targeted optimisation. The work demonstrates the potential of natural fibre-based materials for fin leading edges in the primary structures of sounding rockets on the highest thermally stressed components. The findings of this study offer a foundation for further application of wooden materials in space engineering levelling the path for a bioeconomy in space.

Keywords Wood-based, Renewable resources, Ablation, Thermal protection, Experimental, Arc-heated wind tunnel

List of symbols

A_{intact}	Intact cross-sectional area, mm^2
A_{max}	Maximal cross-sectional area, mm^2
$A_{original}$	Original cross-sectional area, mm^2
c_p	Specific heat capacity, J/kgK
ρ	Density, g/cm^3
h_0	Total enthalpy, MJ/kg
λ	Thermal conductivity, W/mK
m	Mass, g
p_s	Stagnation pressure, hPa
T_M	Melting point, °C

Abbreviations

[1]Institute of Aerospace Engineering, Dresden University of Technology (TUD), 01062 Dresden, Germany. [2]Supersonic and Hypersonic Technologies Department, German Aerospace Center (DLR), 51147 Cologne, Germany. [3]Institute of Natural Materials Technology, Dresden University of Technology (TUD), 01062 Dresden, Germany. [4]Mobile Rocket Base (MORABA), German Aerospace Center (DLR), 82234 Weßling, Germany. [5]Faculty of Space Technologies, AGH University of Krakow, Krakow, Poland. [6]Institute for Structures and Design, German Aerospace Center (DLR), 70569 Stuttgart, Germany. ✉email: raphaela_elisa.guenther@tu-dresden.de

BEXUS	Balloon EXperiment for University Students
CM	Comparative material
DIN EN ISO	International standard (ISO), adopted as European standard (EN), incorporated unchanged into German standards system (DIN)
DLR	German Aerospace Center
ESA	European Space Agency
L2K	Arc heated wind tunnel with 1 MW
L3K	Arc heated wind tunnel with 6 MW
LBK	DLR arc heated facility
Ma	Mach number
MORABA	Mobile rocket base
PT	Preliminary test
PTM	Preliminary test material
REXUS	Rocket EXperiment for University Students
SHAMA	Sustainable heat-protective ablative material (REXUS experiment)
STORT	Flight experiment for: key technologies for high speed return flights of launcher stages
TGA	Thermogravimetric analysis
TPS	Thermal protection system
TPSea	Wood-fibre based thermal protection material developed at TUD
TUD	Dresden University of Technology
VSB	Veículo de Sondagem Booster (eng.: Booster Sounding Vehicle)

The current shift in the space industry towards the development of smaller payloads brings greater flexibility and opens up numerous approaches and opportunities for the development of innovative launch vehicles[1]. In the context of a growing bioeconomy, renewable resources are of interest for the space industry. They have the potential of being future substitute materials towards a CO_2-neutral economy, decreasing debris in space and on Earth, and paving the way to a circular space economy. The ESA Green Agenda emphasises this motivation by focussing on the importance of reducing the environmental impact of space systems[2].

The utilisation of wood and wood-based materials in space applications remains a relatively recent development[3]. Despite the paucity of literature on the subject of wood-based materials for space applications, it is evident that these materials have been applied in aviation more frequently. In space applications, wood has mainly been used for structural, modelling or shock-absorbing purposes. Its use for thermal protection or insulation has been considered and reported in only a few cases, and the available evidence is limited[3].

Castanié et al. provide a broader basis for considering wood and plywood as eco-materials for sustainable mobility[4]. The utilisation and application of wood as a structural material in aviation is well-documented. This can be evidenced by its employment in the main frame of the Kitty Hawk[5], as a sandwich material or as a fuselage and structure material from spruce, birch, fir, ash or balsa wood in the "Hughes H-4 Hercules" and the "De Havilland DH-98 B/TT Mk. 35 Mosquito"[6,7]. In the context of increased material knowledge and material shortages experienced during World War II, wood was retained as a viable material in the aerospace sector[5]. This led to the utilisation of plywood in the inaugural manned rocket, the "Bachem BA 349", marking a significant advancement in aerospace engineering[8–10]. The "Rheintochter" flak rocket further exemplifies this transition, with all its control surfaces being crafted from varnished plywood[11–13], underscoring the material's durability and versatility. Notably, the rocket-powered interceptor "Bereznyak-Isayev BI-1" structural framework was also constructed using plywood[14,15]. In space applications wood is frequently selected for wooden mock-ups and models mainly due to its inherent machinability. A notable example of this application is the red oak replica of the DS2 geometry for the SPRITE mission[16]. Further, the utilisation of wood in satellites is pioneered in the LignoStella project, which led to the development of "LignoSat" and space exposure tests of hardwood species onboard the "Kibo" Module of the International Space Station[17–19]. The WISA Woodsat project also explores the durability of WISA-Birch plywood in space environments[20]. As a shock-absorbing material balsa wood was applied onboard the Ranger 3, 4 and 5 spacecraft designed to protect instruments during impact on the Moon's surface[21,22]. As a thermal protection material balsa wood was considered for the tank insulation of the second stage S-IV and third stage S-IVB of the Saturn V launch vehicle, however never applied due to insufficient delivery capacities[23,24]. Impregnated white oak is reported to have been successfully used as thermal insulation in the nose cap of FSW satellites, although this identification remains unconfirmed by the conflicting technical reports and patents available to the authors[25,26].

These examples demonstrate that wood and wood-based materials have a well-documented history in aviation and have been used in a limited number of space applications. However, the reported space applications primarily concern structural components, models, and shock absorption. There are few reports of wooden materials being used directly for thermal protection or insulation, and in some cases, such as the reported use of white oak, the available evidence is inconclusive. While initial studies have begun to address the development and laboratory testing of bio-based thermal protection materials[27,28], the available data does not yet provide a comprehensive assessment of the use of solid wood and wood-fibre materials under flight-relevant conditions, especially for the direct application on sounding rocket fin leading edges.

This study addresses the identified research gap by investigating solid wood and wood-fibre materials as potential materials for hot sounding rocket structures. The methodological approach comprises the identification of candidate material variants and the characterisation of their thermal performance under flight-relevant thermal loads. For a material screening and subsequent selection, thermogravimetric analysis (TGA) is performed, and the thermal conductivity and specific heat capacity are determined. The thermal performance of the selected materials is evaluated through testing in the arc-heated wind tunnel facility L2K. The evaluation

of the L2K test results is conducted through analysis of mass loss, cross-sectional area and surface contours. In order to facilitate comparison and verification, reference materials previously utilised in the context of high-altitude sounding rockets are employed. The novelty of this work lies in the comparative assessment of bio-based material candidates for a specific hot structure application. The study aims to identify promising solid wood or wood-based material variants for hot space structures, especially for an application on fin leading edges, and establish their current state of development.

Motivation

Due to the increasing need to launch smaller payloads and sounding rocket experiments more frequently, a greater demand for small launch vehicles and sounding rockets arises[29], accompanied by an increased consumption of material resources. Most of the launch vehicle's hardware is designed to be non-reusable, due to a low cost and high efficiency approach of the launch vehicle operator. Only the most valuable scientific payload and payload support systems are commonly recovered and refurbished for re-flights, which are marked in red as an example for the VSB-30 two-stage sounding rocket vehicle in Fig. 1. Considering these circumstances, the resource dimension of sustainability[30] for the launch vehicle, especially the use of renewable raw materials and more sustainable manufacturing processes, becomes a compelling issue for components that are disposed after each flight. The hierarchy of the European Union's circular economy categorisation system (R1, Refuse; R2, Rethink; R3, Reduce; R4, Re-use; R5, Repair; R6, Refurbish; R7, Remanufacture; R8, Repurpose; R9, Recycle) can be used as a guide for developing circular and therefore more sustainable space materials[31]. While one approach is to substitute single-use components with multiple-use components from more durable materials (R4, Re-use), the focus of this research is based on substituting single-use components (R1, Refuse) by using raw materials from renewable origin that rot after the active use and merge into nature again (R9, Recycle) within the biological cycle of the circular economy approach[31]. Within the categorisation used here, one approach is to replace single-use components with multiple-use components made from more durable materials (R4, Re-use). The focus of this research is instead on replacing conventional materials in single-use components with raw materials of renewable origin. Where material composition and end-of-life conditions allow, these materials may biodegrade and return to the biological cycle. This intended biological-cycle pathway should be distinguished from R9 (Recycle), which refers to material recycling in the categorisation listed above[5]. Therefore, it is particularly interesting for single-use components to investigate how the potential of natural, renewable materials can be used and optimized in space engineering and on launch vehicles with regard to sustainability aspects. Wood and wood-based materials have rarely been used in space applications to date. However, there are some applications that take advantage of the beneficial properties of these renewable materials in aerospace environments[3].

Various hot structures can be assigned to single-use components, such as the leading edges of stabilising fins, fairings or nose cones. These components are essential structural components for a stable, aerodynamic flight. Therefore, they have to withstand high thermal and mechanical loads, be characterized by high stiffness and at the same time, should have a relatively low mass. Especially on their foremost front end, where high temperatures may arise from gas kinetic effects, these components must be heat resistant and form stable.

A common solution for overheating components, especially for fin leading edges, can be the use of high temperature steel alloys, thermal protection system (TPS) layers or their combination. The steel version needs to be lightweight, thus almost only sheet metal comes into consideration, revealing to be critical in terms of thermal stress relief deformations affecting the vehicle's flight mechanical performance. Layers of TPS around the leading edge need to be relatively thin and hence are rapidly degrading, leaving the underlying structure unprotected during later flight phases. Figure 2 demonstrates both effects for a typical VSB-30 flight, where a combination of steel sheet metal leading edges with an ablative TPS was used.

Consequently, the German Aerospace Center (DLR) Institute of Structures and Design developed special phenolic glass fibre reinforced leading edges, which were introduced by DLR MORABA on all their thermally higher-loaded fin assemblies. Even though this material serves the temperature load as well as the component's major specifications in a more appropriate way, its lack of lightweight design and environmental sustainability as a non-renewable material are immanent.

Here lies the potential of seagrass- and wood-based materials. They are considered for the application as a TPS material on hot structures due to their relatively low density, low thermal conductivity, lightweight construction

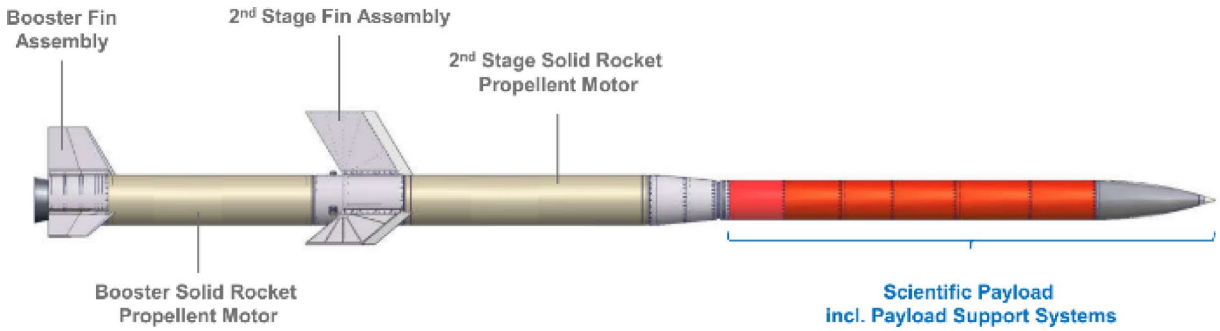


Fig. 1. DLR Mobile Rocket Base (MORABA) VSB-30 two-stage sounding rocket vehicle.



Fig. 2. Thermal load on fin leading edges after 2nd stage burn of DLR MORABA sounding rocket vehicle (left) and 2nd stage fin with steel sheet metal leading edge and ablative TPS recovered after VSB-30 flight operation.

properties, easy handling, good biodegradability and good ablative behaviour. Additionally, sounding rockets are a very suitable test bed to verify component's material and structural concepts for all other launch systems. Therefore, for studying a potential application of bio-based ablative thermal protection materials in space, the fin leading edge of a sounding rocket was chosen as a component for first investigations.

The research was conducted by Dresden University of Technology (TUD) in collaboration with the DLR. As described in the introduction, the DLR STORT flight envelope was taken as a reference, since it is one of the most thermally and mechanically demanding high-altitude research flights of DLR MORABA[32]. Thus, the limits of the material candidates can be extensively explored. The investigation will consider solid wood and wood-fibre materials to identify preferred material variants for an application on fin leading edges of sounding rockets. For comparison, a phenolic glass fibre reinforced material (comparative material 1, CM-1, 2.07 ± 0.1 g/cm^3) and a high temperature steel alloy (comparative material 2, CM-2, 7.9 g/cm^3), which are already applied on sounding rockets, are used. To this end, the same requirements shall be placed on the potential substitute material as applied to currently used materials. This is the first step towards a new structural system based on bio-based materials. The goal should be a differently designed structure with exchangeable and reusable parts. The fin is an example structure that enables relatively simple learning steps and tests. These initial investigations and tests serve to determine the status quo and start subsequent systematic development steps. After successful testing, the aim is to use the findings from the investigation for further material developments, including for applications beyond space technology.

Requirement specification

For the requirement specification three aspects are taken into consideration. The requirements of fin leading edges in general, optional requirements of fin leading edges from natural origin, and additional requirements for natural fibre-based fin leading edges. For all three requirement types, the substitute material should be able to withstand the same requirements as the materials used to date by MORABA and thus should fulfil the same functions. Therefore, the thermal material characteristics of the comparative materials CM-1 and CM-2 are taken as benchmark values with thermal conductivities of CM-1 (0.4 ± 0.1 W/mK) and CM-2 (15 W/mK) and the specific heat capacities of CM-1 (> 850 J/kgK) and CM-2 (500 J/kgK).

General requirements for fin leading edges, formulated by DLR MORABA are:

- The fin leading edges shall be fail-safe at all times during the mission.
- The fin leading edges shall support aerodynamic loads of the STORT mission in medium range and thermal loads in high range.
- The fin leading edges geometry and integrity shall be maintained over a long period of the flight.

Optional requirements for fin leading edges from natural origin, formulated by DLR MORABA are:

- The bio-based fin leading edge shall have a relatively low mass.
- The bio-based fin leading edge shall provide an improvement in flight stability.
- The bio-based fin leading edge shall reduce the flutter behaviour.
- The bio-based fin leading edge shall reduce the polar moment of inertia.
- The bio-based fin leading edge shall have relatively low production costs.

Additional requirements for bio-based fin leading edges identified by TUD are:

- Bio-based fin leading edges shall have high material strengths and densities to maintain structural integrity under mechanical and high thermal loads.
- Bio-based fin leading edges shall have low thermal conductivity and high thermal resistance to prevent heat transfer throughout the fin structure.
- Bio-based fin leading edges shall maintain their geometry.

The requirements presented above guide the material design from a technical as well as an application perspective in the next steps.

Material screening and selection

The materials to be tested should represent a wide range of material properties within their material type. Thus, the materials can be compared with each other in a more differentiated manner. As natural fibre-based materials, the materials solid wood and wood-fibre materials are selected. As solid woods, both softwoods and hardwoods are selected. Among the possible tropical and native woods, native wood species are preferred for an application on a European sounding rocket, as they are readily available in Europe and reduce CO_2 emissions during harvesting, transport and logistics. Therefore, only regional, native wood species are considered in the material selection. In the case of wood-fibre materials, industrial material (I-WBM) is compared with material developed by TUD (TPSea-0, TPSea-1 and TPSea-C)[33]. Thereby a special focus is placed on a newly developed wood-fibre material TPSea-C with a patented recipe containing wood fibres, seagrass fibres *Zostera marina* and a bio-based flame retardant[28,34,35]. This material was promising because of its good thermal resistance and easy manufacturability. Within the experiment SHAMA (Sustainable Heat-protective Ablative Material) TPSea-C has been launched as part of the REXUS/BEXUS programme onboard REXUS 34[27].

To identify most suited wood-fibre materials for an application on fin leading edges, screening tests were carried out for the test material selection. As the main stress on the leading edge of the fin is caused by thermal loads and the temperature resistance of the fin edge is a general requirement, analyses to characterize thermal material properties form the basis for the selection of the material.

Preliminary test

The evaluation of a preliminary test (PT) serves as experimental basis. Test specimens made of solid woods oak (*Quercus petraea, Q. robur*, PT-Oak) and mahogany (Andiroba *Carapa guianensis*, PT-Mahogany), specimens of a preliminary test material 1 (PTM-1) based on carbon fibres and the comparative material 1 (CM-1) based on a phenolic glass fibre reinforced composite were each tested once in the arc-heated wind tunnel L2K of the Institute of Aerodynamics and Flow Technology, Supersonic and Hypersonic Technologies (DLR). In addition to a mass and a cross-sectional area analysis, a microscopic analysis of micrographs was conducted.

The tests show for PTM-1 (1.55 ± 0.05 g/cm^3) a residual mass of 87.08% and for CM-1 (2.07 ± 0.1 g/cm^3) a residual mass of 92.44%. The residual mass of PT-Oak (49.47%) is lower than that of PT-Mahogany (59.66%) even though the test specimen densities are with 0.83 ± 0.06 g/cm^3 (oak) and 0.85 ± 0.06 g/cm^3 (mahogany) comparable. A thorough analysis of the cross-sectional geometry of the test specimens revealed the residual cross-sectional areas differ slightly by 0.8%, with PT-Mahogany showing a residual area of 51.11% and PT-Oak of 50.31%. The proportion of char layer is 5% greater in PT-Mahogany than in PT-Oak. Even though the test specimen densities are comparable, a clear correlation between the anatomy of the wood species and their behaviour under thermal load can be seen. As seen in Fig. 3, the large differences in pore size between earlywood and latewood, combined with the comparatively broad wood rays of PT-Oak, result in more pronounced and locally heterogeneous thermal degradation. In contrast, PT-Mahogany exhibits a lower and more spatially uniform degradation, which can be attributed to its narrower wood rays and more homogeneous pore distribution. The orientation of the wood rays appears to have a significant influence on the progression of thermal degradation.

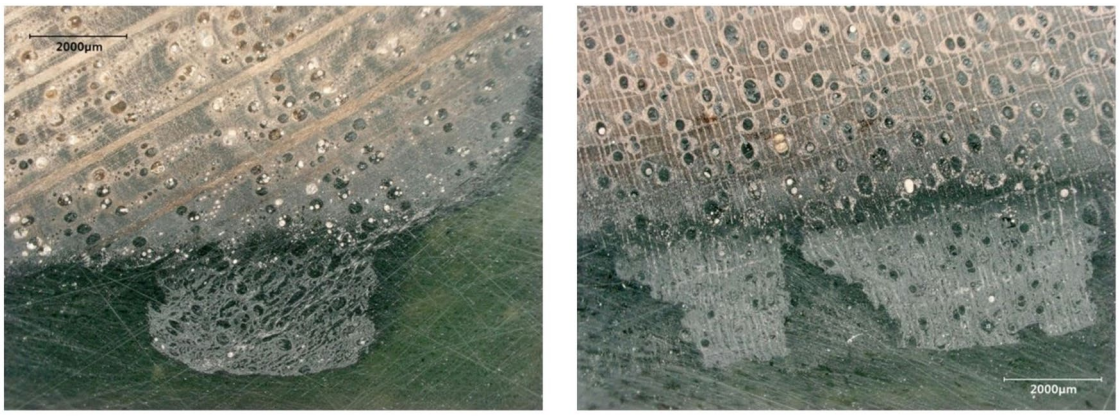


Fig. 3. Microscopic image of cross-section of PT-Oak (left) and PT-Mahogany (right) at 30 × magnification with minimised glare.

In the investigated cross-sections, the oblique orientation of the rays provides preferential pathways for heat transport into the material, as the heat flux encounters fewer cell walls along the ray direction. Consequently, thermal degradation progresses more rapidly along these pathways, resulting in increased material loss at the upper surface. This effect is particularly pronounced in the PT-Oak specimen.

Microscopic analysis further reveals the formation of a porous carbonised layer and an underlying pyrolysis zone in both materials. However, both layers are thicker in PT-Mahogany, with an approximately 2500 µm thick porous carbon layer and a 1200 µm pyrolysis zone, compared with approximately 2000 µm and 500 µm, respectively, for PT-Oak (see Fig. 3). Despite its greater thickness, the carbonised layer of PT-Mahogany exhibits higher structural integrity, which can be attributed to its finer and more homogeneous pore structure. The orientation of the specimens' wood grain resulted in the thermal load being applied predominantly perpendicular to the grain direction of the solid wood. As discussed by Niemz and Sonderegger[36], the thermal conductivity of wood perpendicular to the grain is approximately half that parallel to the grain. This orientation is therefore advantageous for applications in which heat transfer from a thermally exposed leading edge into the interior of the component should be minimised.

Thermogravimetric analysis (TGA)

Particular focus was placed on a TGA as a fundamental screening tool, which provides information on the char yield and pyrolytic behaviour of a material by determining the change in mass of a test material as a function of temperature and time. The TGA was performed with the test materials listed in Table 1 each with two test specimens, given the constrained testing capacity. While this number was considered sufficient for identifying general trends, the limited sample size is acknowledged as a limitation. In addition to three wood-based materials produced at TUD (TPSea-0, TPSea-1 and TPSea-C), an industrially manufactured wood-based material (I-WBM) was selected to serve as a reference material for the wood-based materials. Despite the good performance of PT-Mahogany in the preliminary test, further investigations focused on wood species native to Europe and that are readily available. Consequently, oak *Quercus petraea, Q. robur* (hardwood) and larch *Larix decidua, Larix* spp. (softwood) were selected for the TGA.

The measurements were carried out in two steps:

1. The pre-dried test specimens were heated in the TGA test device (LECO TGA 701) with a temperature increase of 15 K/min from 25 to 105 °C.
2. The test specimens were heated from 105 to 1000 °C at 40 K/min.

During the measurement, a nitrogen atmosphere with a volume flow of 3.5 l/min prevailed in the measuring device.

The visual test results are displayed each before and after the analysis in Fig. 4. The black and cracked or porous surfaces of the TPSea-1 (top row left) and I-WBM samples (top row right) can be seen. The surfaces of the TPSea-C (middle row left) show light-coloured, mineral deposits. The test specimens of TPSea-0 (middle row right) show a significant loss in volume and a dark, charred surface. All wood-fibre materials retain their materials' cohesion. The test specimen of the solid wood oak (bottom row left) and larch (bottom row right) are structurally very degraded or disjointed. A partially charred and ashen, fragile surface can be seen.

A clear mass loss for all test specimens at 1000 °C can be seen in Fig. 5. The pre-drying results in a negligible mass loss due to the evaporation of water, as the data curves are nearly constant until 120 °C. Therefore, it can be deduced that the mass losses shown are exclusively caused by the ingredients of the test materials. The test specimens made of solid wood retain their mass up to a temperature of about 200 °C, after which it drops very steeply to less than 12 ± 0.006% (larch) and less than 18 ± 0.009% (oak). The TPSea-0 test specimens have slightly higher residual mass percentages above 20 ± 0.01% compared to the solid wood test specimens. The I-WBM and TPSea-1 test specimens still have 32 ± 0.009% to 35 ± 0.01% of their original mass when they reach 1000 °C. Within the same material, the curves of mass loss are approximately similar. Comparing the curves of TPSea-0 and TPSea-1, it becomes evident that the use of flame retardant has a positive effect on mass loss. With above 42 ± 0.012%, the TPSea-C test specimens show the highest residual mass ratio. This result can be explained by the material's composition. The natural salts, sandy residues and suspended matter contained in the seagrass fibre have high melting points (sodium chloride/ salt: $T_M \sim 801$ °C[37], quartz sand: $T_M \sim 1713$ °C[38]), slowing down the materials' decomposition and thus acting as natural flame retardants. These not decomposed components form the light-coloured, mineral deposits as seen in Fig. 4 on the test specimen surface.

Test material	Material specifications	Further information	Number of test specimens
Oak	Solid wood, hardwood	*Quercus petraea, Q. robur*	2
Larch	Solid wood, softwood	*Larix decidua, Larix* spp.	2
I-WBM	Industrial wood-based material	Contains flame retardant (proportion unknown)	2
TPSea-0	Wood-based material *	100% Wood fibre, flame retardant free	2
TPSea-1	Wood-based material *	100% Wood fibre, 10% Bio-based flame retardant	2
TPSea-C	Wood and seagrass fibre-based material *	Wood fibre, seagrass fibre *Zostera marina*, 10% Bio-based flame retardant	2

Table 1. Test materials for TGA. * Produced at TUD.

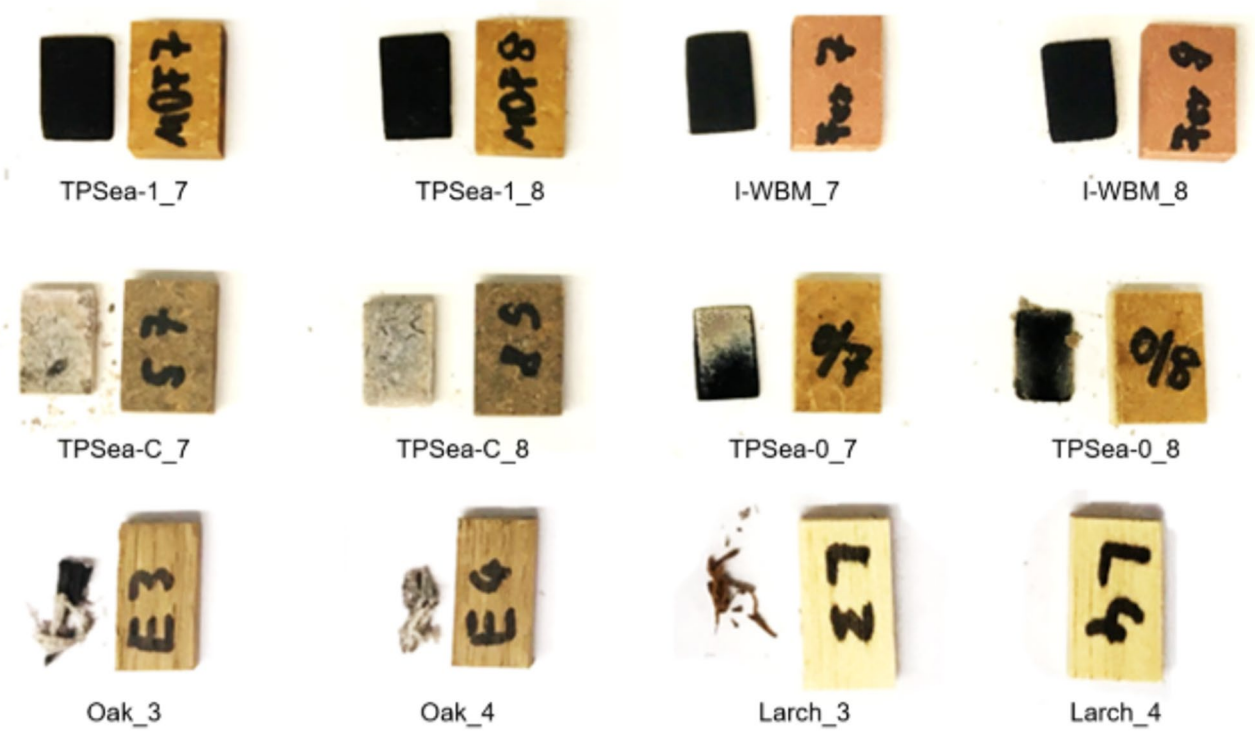


Fig. 4. Test specimens each before (right) and after (left) TGA.

Thermal material characterisation

For the newly at TUD developed wood-based materials the density (in accordance with DIN EN 323:1993-08 with KERN precision scale), thermal conductivity and specific heat capacity (in accordance with DIN EN ISO 22007-2:2015 with Hot Disk® TPS instrument) were determined for the material screening. The results of the characterisation and literature values ([39]) for the remaining materials are shown in Table 2.

The thermal conductivities of all wood-fibre materials are only slightly lower than the thermal conductivity of CM-1, but up to 40 times lower than the thermal conductivity of CM-2. This means that the natural fibre-based materials insulate heat better and transfer less heat to the fin when used in fin leading edges. Compared with literature values of $\lambda = 0.18$ W/mK according to DIN EN ISO 10,456 for wood-fibre boards with densities of 0.8 g/cm^3[40], the analysed materials have higher thermal conductivities.

The values of the specific heat capacity of all analysed materials are very similar. The specific heat capacities of the wood-fibre materials are up to 1.7 times (CM-1) or three times (CM-2) as large as those of previously used materials. This means that the natural fibre-based materials can store heat better or have a lower temperature rise in the material. For the use of these materials in fin leading edges, more heat would be required to heat the material compared to the fin leading edge materials used so far. Compared to literature values of $c_p = 1700$ J/kgK according to DIN EN ISO 10,456 for wood-fibre boards with densities of 0.8 g/cm^3[40], the analysed materials have lower specific heat capacities.

Material selection

Based on the screening tests, the requirement analysis and especially under consideration of the TGA results, materials for testing in the arc-heated wind tunnel L2K were selected on the basis of four criteria:

- *Criterion 1: Test capacity determines the number of specimens*:

The total number of specimens to be selected is based on the maximum test capacity of the L2K.

- *Criterion 2: Wide range of test materials*:

The materials to be tested should represent a wide range of material properties within their respective material types. This allows for a more nuanced comparison between the materials.

- *Criterion 3: For solid wood – regional origin, source, bulk density and anatomical structure*:

Of the possible tropical and native wood species in Europe, native wood species are preferred for use in a European high-altitude research rocket, as they are readily available in Europe and reduce CO_2 emissions during harvesting, transport and logistics. Consequently, only regional, native wood species are considered as part of the material selection process. Attention must be paid to the origin of the solid wood. Depending on

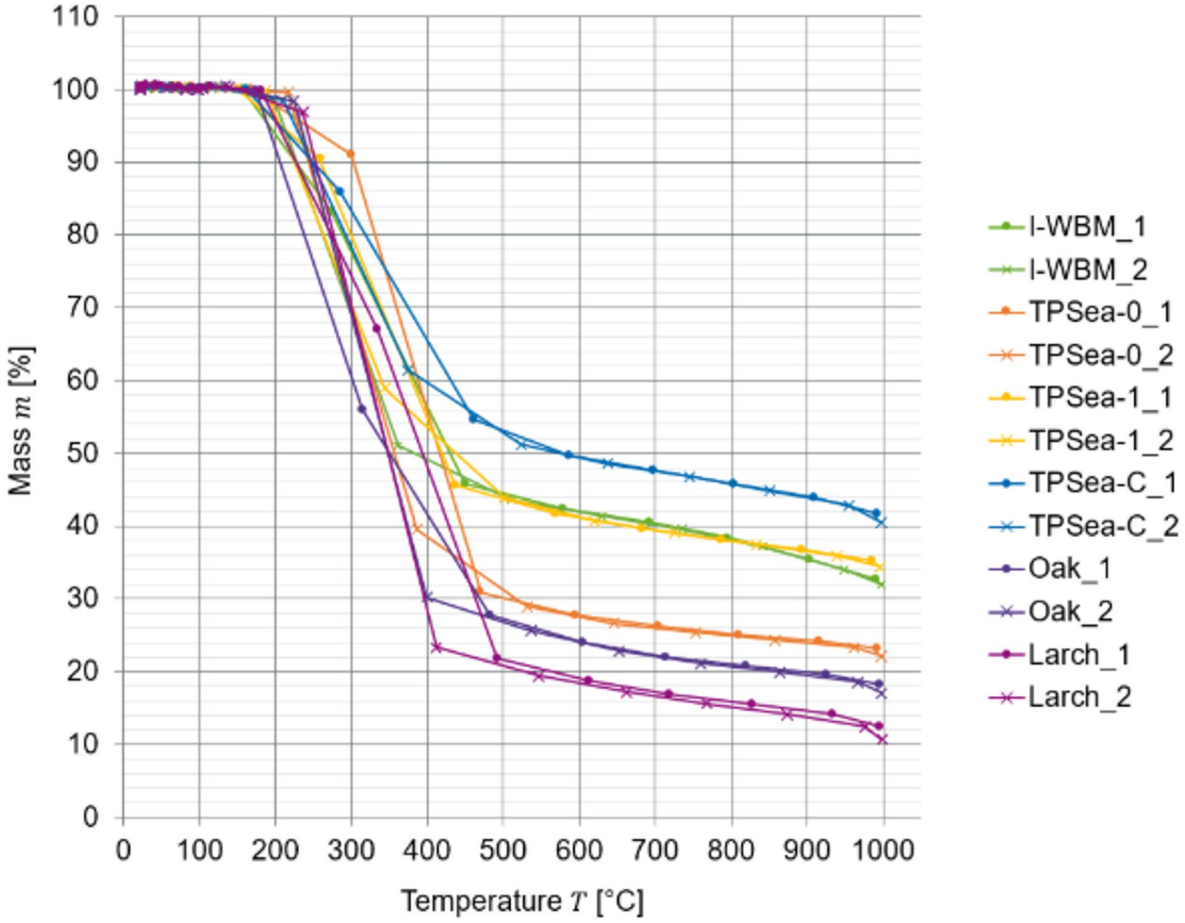


Fig. 5. Test results of TGA.

Material	Density ρ [g/cm^3] of test specimen	Thermal conductivity λ [W/mK]	Specific heat capacity c_p [J/kgK]	Number of test specimens per test
Oak	0.66 ± 0.06 $^+$	0.166 ± 0.005[39]	–	3
Larch	0.55 ± 0.06 $^+$	0.114 ± 0.003[39]	–	3
I-WBM	0.80 ± 0.05 $^+$	0.225 ± 0.011	1446.0 ± 173.52	3
TPSea-1	0.87 ± 0.15 $^+$	0.353 ± 0.018 (plane)	1467.7 ± 176.12	3
TPSea-C	0.89 ± 0.15 $^+$	0.252 ± 0.013	1493.2 ± 179.18	3
CM-1	2.07 ± 0.1	0.4 ± 0.1	> 850	–
CM-2	7.9	15	500	–

Table 2. Properties of test materials for thermal characterisation. $^+$ Measurements at TUD under standard climatic conditions (DIN 50014-20/65–1: 20 °C ± 1 °C, 65% ± 3% relative humidity, 12 ± 1.5% wood moisture content).

the environmental and weather conditions at the site, the timber may grow at different rates and consequently possess different properties. Material density plays a key role in determining mechanical and thermal properties, as well as the structural integrity and flight stability of the material used in fin leading edges. A higher density implies superior mechanical properties and provides more mass per unit volume, which is available for ablative and pyrolytic processes. Consequently, materials with high bulk densities are to be preferred. From a wood anatomical perspective, solid woods with long fibre lengths, thick fibre walls and an even distribution of vessels across the cross-section are preferred.

- *Criterion 4: Wood-fibre materials – flame retardant, bulk density and bio-based composition*:

Based on the requirements analysis, wood-fibre materials with a high degree of pulping and a high average bulk density are selected. Preference is given to flame-retardant materials containing thermosetting binders with a high melting point, which also incorporate flame retardants. The focus for the materials produced at TUD is on achieving the highest possible proportion of natural, bio-based components.

Due to the limited capacity of the testing facility, a total of six materials were selected for L2K testing (criterion 1). Of these, three are to be solid wood and three are to be wood-fibre materials to achieve a wide range of test materials (criterion 2). Because hardwoods have higher average strengths and densities[41,42], two hardwoods (oak and birch) and one softwood (larch) were chosen. Although the results of the preliminary test show that oak is not particularly well suited due to its ring-porous structure, it was selected for further testing as it is a widely available solid wood native to Europe and has an average high density (literature value: 0.71 ± 0.064 g/cm^3[41]). Birch was selected as a semi-ring-porous timber primarily because of its high elasto-mechanical properties. Larch, with a density of 0.6 g/cm^3 ± 11%[41] (literature value), is among the denser and mechanically stronger European softwoods commonly used for structural and engineering applications. The solid woods for the test specimens were selected from the TUD's collection of materials, with particular attention paid to a relatively uniform structure, free from imperfections (criterion 3). The test specimen densities can be found in Table 4. For the wood-based materials, an industrially produced fibreboard material I-WBM was selected, which was developed for increased fire protection requirements in non-load-bearing interior applications in dry areas. In the context of the investigations, it represents an industrial comparative material. The TPSea-1 and TPSea-C materials from TUD were also selected. They contain flame retardants, are composed mainly of natural ingredients and have high average bulk densities (see Table 2; criterion 4). The test specimens for L2K of the selected materials are shown in Fig. 6.

Wind tunnel testing

In the scope of testing, the test facility, the test conditions and test specimens are described below. Further, test results are presented.



Fig. 6. Test specimen of selected material.

Test facility—Arc-heated wind tunnel L2K

The arc-heat wind tunnel facilities LBK of DLR are certified by ESA as a European key facility for testing and qualification of thermal protection systems. The LBK facilities consist of two nearly independent test legs, called L2K and L3K. The setup of the facilities is schematically plotted in Fig. 7. The two legs share a common system of vacuum pumps and exhaust gas cleaning as well as the low-pressure cooling cycle for the test chamber and the heat exchangers in the diffusors. Apart from this, the facilities can operate independently as each is equipped with their own power and gas supply, arc heater cooling systems and controls. The L2K facility is equipped with a Huels-type arc heater for gas mass flow rates between 5 and 75 g/s. With a maximum power of 1.4 MW moderate specific enthalpies up to 10 MJ/kg are achieved at a gas mass flow rate of 50 g/s, which corresponds to a reservoir pressure of about 1500 hPa. As the working gases, air, nitrogen, argon or mixtures thereof e.g. for Martian (CO_2/N_2) or Titan (N_2/CH_4) atmospheres can be used.

Hypersonic free stream velocities are provided by a convergent-divergent nozzle. The nozzle's expansion part is conical with a half angle of 12°. Different throat diameters from 14 to 29 mm are available and can be combined with nozzle exit diameters of 50 mm, 100 mm, and 200 mm. Consequently, the facility setup can effectively be adapted to particular necessities of a certain test campaign[43–45].

Test condition and test specimens

The test condition was chosen to represent the case of maximum total enthalpy encountered during the projected STORT flight trajectory which occurs at an altitude of approximately 41.5 km at a flight Mach number of 8.6. At this point the vehicle experiences a total enthalpy of about h_0 = 4.048 MJ/kg at a stagnation pressure of $p_s \approx$ 254 hPa. With these values, the parameter

$$h_0 \bullet \sqrt{p_s} \approx 64.5 \tag{1}$$

can be calculated as a reference value for the thermal load, when h_0 is entered in the unit MJ/kg and p_s in hPa. This parameter can then be used as a similarity parameter for determining the wind tunnel conditions. Furthermore, it has to be considered that the flow in L2K is in thermal and chemical non-equilibrium with a rather high portion of atomic oxygen from dissociation in the arc-heater, when air is used as a test gas, whereas in real flight, the portion of atomic oxygen is very small (<<1%). In order to account for these factors, the condition in Table 3 with a mixture of 96% nitrogen and 4% air was used for the wind tunnel tests.

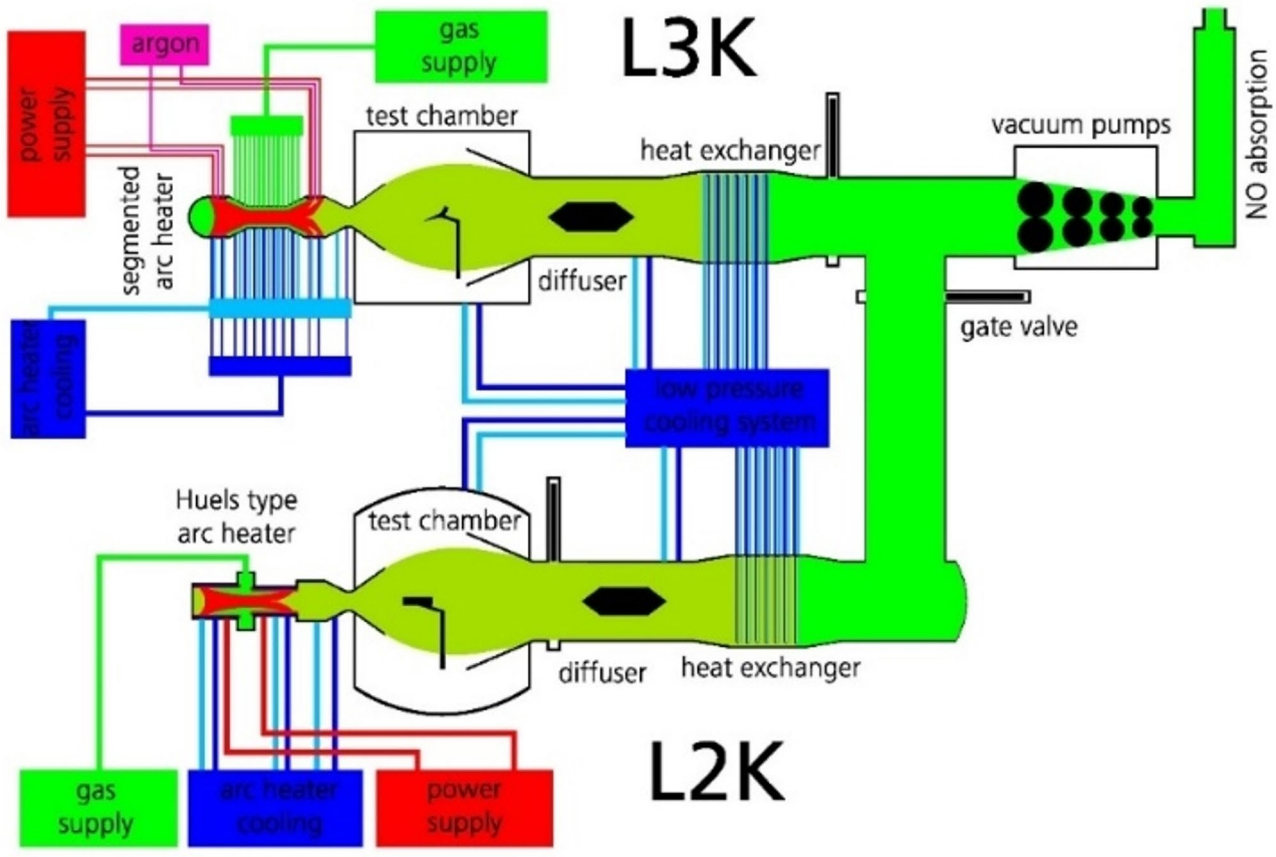


Fig. 7. Schematic overview of the arc-heated wind tunnel facilities LBK.

Flow parameter	Value
Total gas mass flow [g/s]	50
Air mass flow [g/s]	2
Nitrogen mass flow [g/s]	48
Total enthalpy [MJ/kg]	6.85
Stagnation pressure [hPa]	89
$h_0 \cdot \sqrt{p_s}$	64.6
Nozzle configuration (throat/exit diameter) [mm]	29/100
Distance from nozzle exit [mm]	120
Test duration [s]	120

Table 3. Test conditions for L2K experiments.

Material	Density ρ [g/cm^3] of test specimen	Material specifications	Further information	Number of test specimen
Oak	0.66 ± 0.06 $^+$	Solid wood, hardwood	*Quercus petraea, Q. robur*	1
Birch	0.61 ± 0.06 $^+$	Solid wood, hardwood	*Betula pendula*	1
Larch	0.55 ± 0.06 $^+$	Solid wood, softwood	*Larix decidua, Larix* spp.	1
I-WBM	0.80 ± 0.05 $^+$	Industrial wood-based material	Contains flame retardant (proportion unknown)	3
TPSea-1	0.87 ± 0.15 $^+$	Wood-based material *	100% Wood fibre, 10% Bio-based flame retardant	3
TPSea-C	0.89 ± 0.15 $^+$	Wood-based material *	Wood fibre and seagrass fibre *Zostera marina*, 10% Bio-based flame retardant	3

Table 4. Test specimen details for L2K testing. $^+$ Measurements at TUD under standard climatic conditions (DIN 50,014–20/65–1: 20 °C ± 1 °C, 65% ± 3% relative humidity, 12 ± 1.5% wood moisture content). * Produced at TUD.

Table 4 shows the test specimens details and corresponding test specimen density for L2K testing. All test specimens consist entirely of solid material. The test specimens from the solid woods birch, oak and larch were tested once, as these materials showed the highest degradation. The test specimen showing the least degradation after one test, were tested three times in total. Thus, reliability was increased in the testing. The materials tested three times include I-WBM, TPSea-1 and TPSea-C.

The test specimens do not have temperature sensors integrated into the sample structure. The sample geometry used results from the defined fin leading edge geometry. During the tests, the test specimens are clamped into a cooled sample holder, which is fixed in the test chamber of the L2K. A water-based cooling system ensures uniform removal of heat from the sample holder during measurements and guarantees firm clamping at the applied thermal loads. The selected test conditions replicate the thermal loads of the STORT mission. However, the test facility L2K can solely simulate the thermal loads and cannot replicate the mechanical, shock and vibration loads that occur during a real launch[43,46]. This can be considered a limitation.

Test results

The boundary layer that forms around the test specimen during testing is seen in Fig. 8. In the upper half of the image, the mechanical surface erosion of the ablation shows the removal of a material particle that is carried away from the test specimen by the wind tunnel flow. The test specimen tips of TPSea-C and oak are shown on the right side of Fig. 8. At the TPSea-C test specimen the annealing of the test specimen tip and the formation of melt beads from the resins and mineral components contained can be seen. The pointed shape and straight fin leading edge were maintained throughout the test period. The tip of the oak test specimen decomposes irregularly compared to TPSea-C and does not form a straight leading edge. The pointed test specimen shape cannot be maintained over the test duration of 120 s. A detachment of porous carbon can be seen on the upper part of the test specimen.

The grey background of the temperature measurements of 1- and 2-colour pyrometer in Fig. 9 illustrates the test time of 120 s. At the sample tip of TPSea-C, the temperature initially rises from 1500 °C to a maximum of 2300 °C and remains relatively constant over the test duration. In contrast, the temperature measurement of the oak specimen shows clear fluctuations. This is due to a stronger degradation of the material at the test specimen tip, where the focus of the measuring spot of the temperature measurement is lost after flaking of material and is blurred or no longer on the specimen. From t = 20 s onwards, flaking of material can be detected due to strong temperature fluctuations. After 110 s, the 2-colour pyrometer no longer measures any results and drops abruptly from 2400 °C to its starting range of 1000 °C. This is also associated with the loss of the measuring range and can be explained by the loss of the measuring spot on the material surface. The two exemplary measurement results

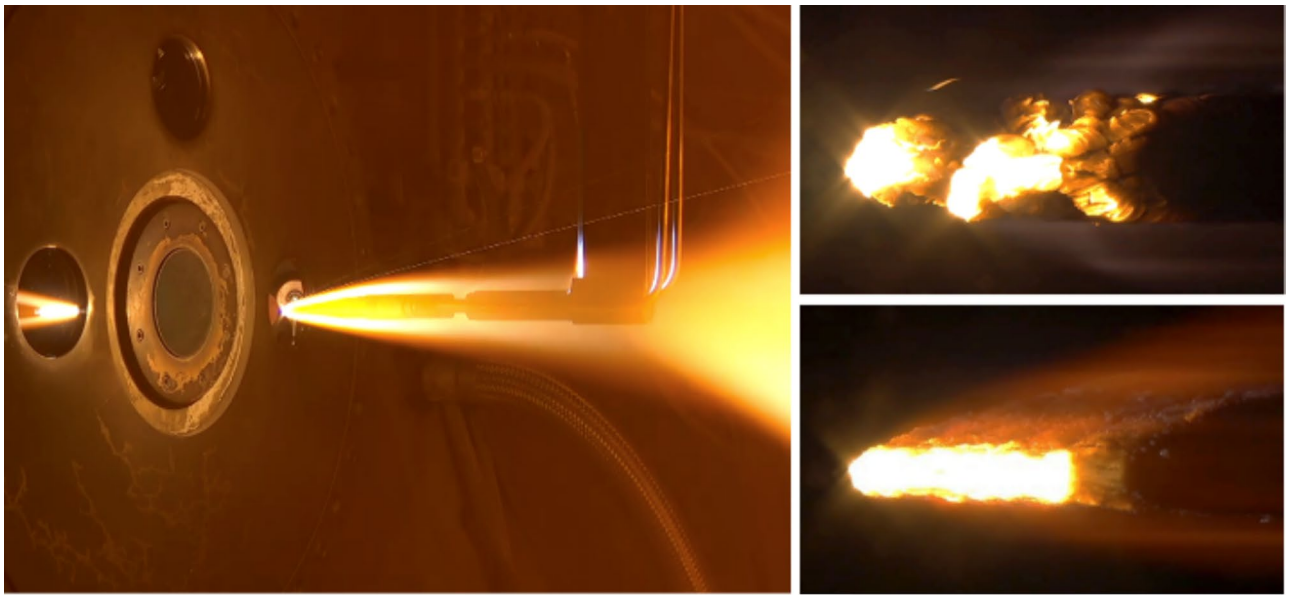


Fig. 8. Test specimen during testing (left), test specimen tips of oak (top right) and TPSea-C (bottom right) at 120 s.

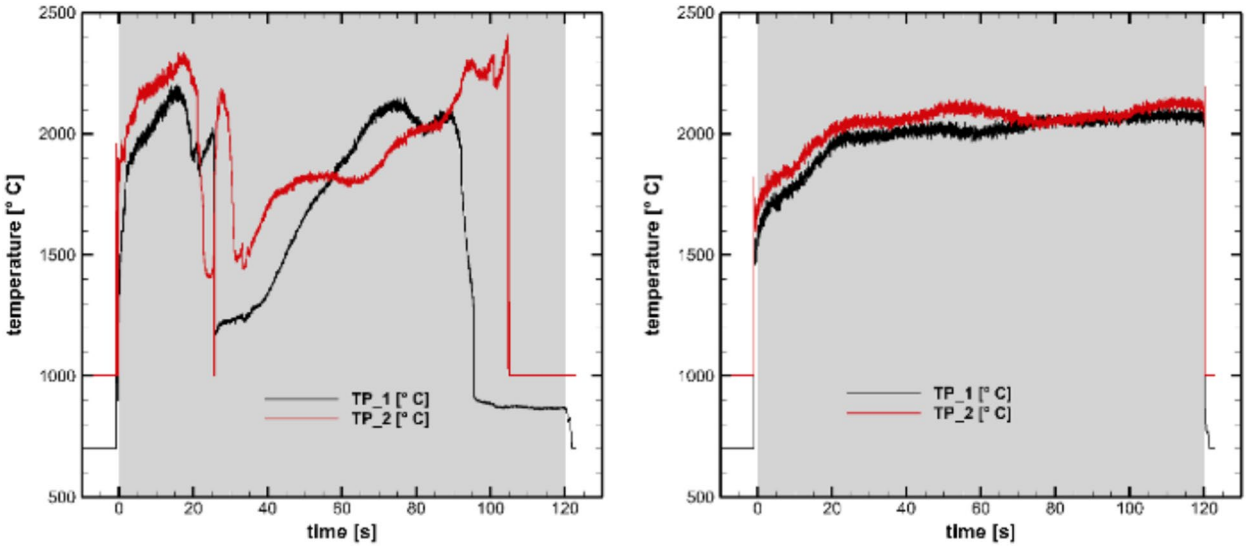


Fig. 9. Temperature measurements of an oak (left) and TPSea-C (right) test specimen.

of the temperature at the specimen tip clearly show the differences between the specimen materials in the wind tunnel tests.

Figure 10 shows a test specimen after testing on the left side. The thermographic images on the right side of Fig. 10 show the strong thermal load at the test specimen tip, which decreases towards the test specimen holder. The test specimen flanks have lower temperatures than the top and bottom. The TPSea-C test specimen has a uniform, continuous tip contour after t = 60 s as well as t = 120 s, while oak has a blunt tip with discontinuous progression.

Post-test analysis

The analyses for evaluating the tests in L2K consist of a mass analysis, a cross-sectional area analysis and a contour analysis, which are described below. The contour analysis method was not available in the preliminary test and was therefore not carried out for the materials CM-1, PTM-1, PT-Oak and PT-Mahogany. A summary of the test specimens used for the post-test analysis can be found in Table 5.

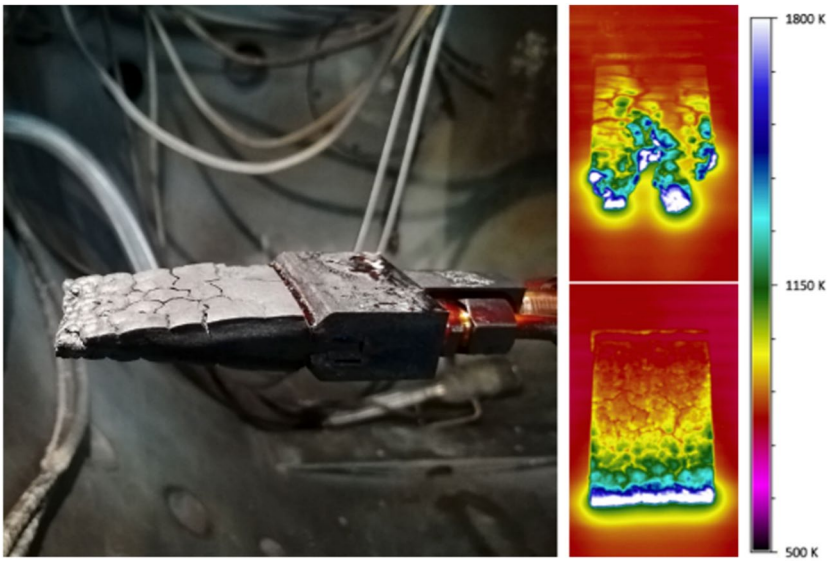


Fig. 10. Test specimen after testing (left), thermographic images of oak (top right) and TPSea-C (bottom right) at 60 s.

Material	Density ρ [g/cm³] of test specimen	Number of analysed test specimen		
		Mass analysis	Cross-sectional area analysis	Contour analysis
Oak	0.66 ± 0.06 ⁺	1	1	1
Birch	0.61 ± 0.06 ⁺	1	1	–
Larch	0.55 ± 0.06 ⁺	1	1	–
I-WBM	0.80 ± 0.05 ⁺	3	3	–
TPSea-1	0.87 ± 0.15 ⁺	3	3	1
TPSea-C	0.89 ± 0.15 ⁺	3	3	1
PT-Oak	0.83 ± 0.06 ⁺	1	1	–
PT-Mahogany	0.85 ± 0.06 ⁺	1	1	–
CM-1	2.07 ± 0.1	1	–	–
PTM-1	1.55 ± 0.05	1	–	–

Table 5. Overview of test specimen for post-test analysis. ⁺ Measurements at TUD under standard climatic conditions (DIN 50,014–20/65–1: 20 °C ± 1 °C, 65% ± 3% relative humidity, 12 ± 1.5% wood moisture content).

Mass analysis

The mass of the test specimens was determined before and after the tests in L2K with a precision balance. For the mass analysis all mass fractions were related to a test time of t = 120 s. These are shown together with the results from the preliminary test in Fig. 11, sorted by ascending mass fraction after the test. In addition, the corresponding test specimen densities are displayed.

The wood-fibre materials of the test specimens from I-WBM, TPSea-1 and TPSea-C show higher residual masses from 53.2 to 62.0% than the solid woods, whose residual masses range between 34.0 and 38.1%. However, compared to the results of the composites PTM-1 and CM-1 in the preliminary test, the natural fibre-based materials have a significantly lower residual mass than the composites PTM-1 and CM-1 with residual masses of 87.1% and 92.4%. TPSea-C surpasses the solid woods PT-Oak (49.5%) and PT-Mahogany (59.6%) tested in the preliminary test. All test specimens of the same material have comparable results and therefore validate the material behaviour well. Their results are summarised by their mean value in Fig. 11. The TPSea-C test specimens show between 2.4 and 4% higher residual masses than PT-Mahogany and are characterised by the highest residual masses of all tested materials. With a test specimen density of 0.89 ± 0.15 g/cm³, the TPSea-C test samples have a comparable calculated density to the solid wood test specimen PT-Oak (0.83 ± 0.06 g/cm³) and PT-Mahogany (0.85 ± 0.06 g/cm³) from the preliminary test but show a slightly higher residual mass.

Cross-sectional analysis

For the cross-sectional area analysis in the L2K test series the test specimens were cut at a distance of approximately 10 mm from the right sample flank. This distance was chosen because the samples tested in the L2K show a higher and more irregular material loss on the sample flanks. For further analysis, the large test

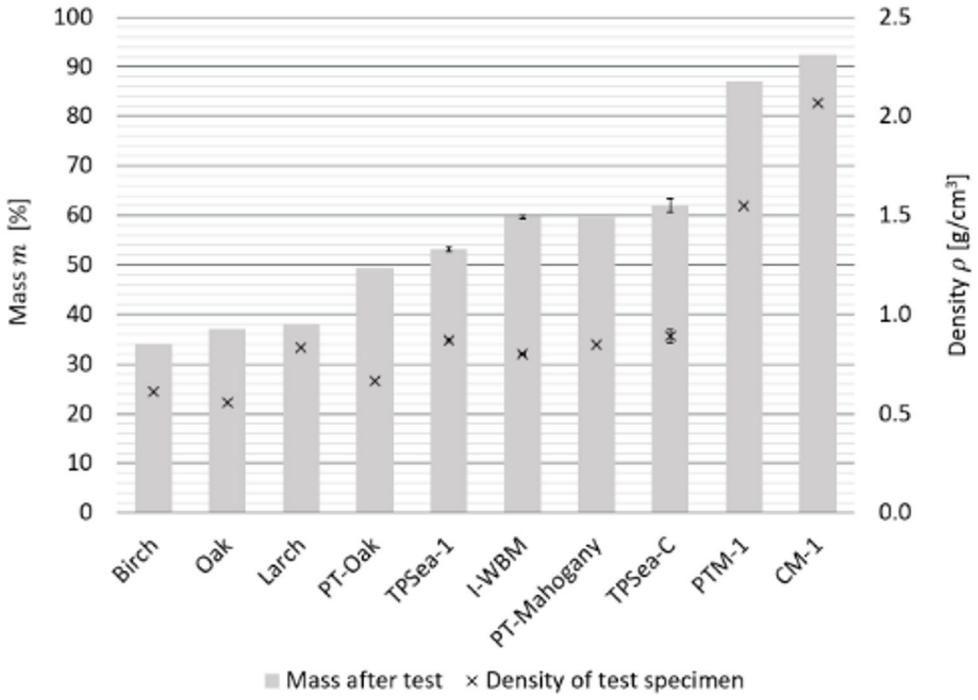


Fig. 11. Results of mass analysis.

specimen part was considered, since the cutting process damaged material parts of the gate more frequently. During the cutting process, it was found that all wood-fibre materials tended to lose less charred material and had a higher structural integrity than the solid woods.

The intact cross-sectional area A_{intact}, which represents the cross-sectional area with virgin material, the maximum cross-sectional area A_{max}, which results from the intact cross-sectional area and the porous char layer, as well as the original cross-sectional area $A_{original}$ are determined with the program ImageJ. Figure 12 shows examples of the superimposed results of the cross-sectional area analysis of TPSea-C and oak compared with the original cross-sectional area $A_{original}$ before the tests in the L2K.

The percentage of cross-sectional area shares related to t = 120 s are shown for all test specimens with the results from the preliminary test sorted by ascending maximum cross-sectional area share in Fig. 13. Analogous to the mass analysis, the corresponding test specimen densities are additionally displayed.

The test specimens made of wood-fibre materials show a higher maximum residual cross-sectional area in the range of 66.1–79.2% than the solid woods, which have residual cross-sectional areas between 35.1 and 51.6%. The test specimens made of wood-fibre materials have the largest maximum cross-sectional areas of all tested materials after the test. The test specimens of the preliminary test are in line with the cross-sectional ratios of the solid woods. It is noticeable that the wood-fibre materials have a larger maximum cross-sectional area, but the intact cross-sectional ratios for the wood-fibre material (31.5–47.0%) overlap with the range of the solid woods with 28.0–39.8%. Especially samples from TPSea-C show high maximum residual cross-sectional areas as well as high intact residual cross-sectional areas, which consist of a porous, but still structurally intact, carbon layer.

Contour analysis

The contours of the test specimens have been analysed to provide information on the extent to which the material degraded during the test, allowing conclusions to be drawn about different degrees of degradation for the same test time of 120 s. For the contour analysis, the scans that recorded the contour of the test specimens before and after the test were evaluated and compared with each other. As Fig. 14 shows, the test specimens were scanned in a scan holder with an angle of attack of 35°. Since the samples in the L2K are symmetrically exposed to the wind tunnel flow, only the upper side of the samples, which represents the white part of the sample in Fig. 14, can be used as an example for the contour analysis. To determine a surface contour, the samples were virtually cut along an analysis line, preferably in the centre of the specimen. In this way, a representative cut was made through the sample, which lies in the area of greatest stress on the test specimen.

The contours of the upper surfaces of the test specimens Oak, TPSea-1 and TPSea-C can be seen in Fig. 15 and can be interpreted in the same way as in Fig. 14. The original contour of the top side of the test specimen before the test is marked in black, while the surface contour after the test is marked in red. To the right of the contour curves, the top surfaces of the test specimens are shown with the analysis lines before and after the tests.

In the case of the test specimen with oak, a strong loss of material can be seen at the top of the test specimen, as the red contour line on the right-hand side drops steeply downwards. This means that the scanner no longer saw the top of the specimen but the reference surface. Compared to the black contour, the red contour runs relatively narrow. Some indentations can be seen, which can be explained by the porous carbon layer and the

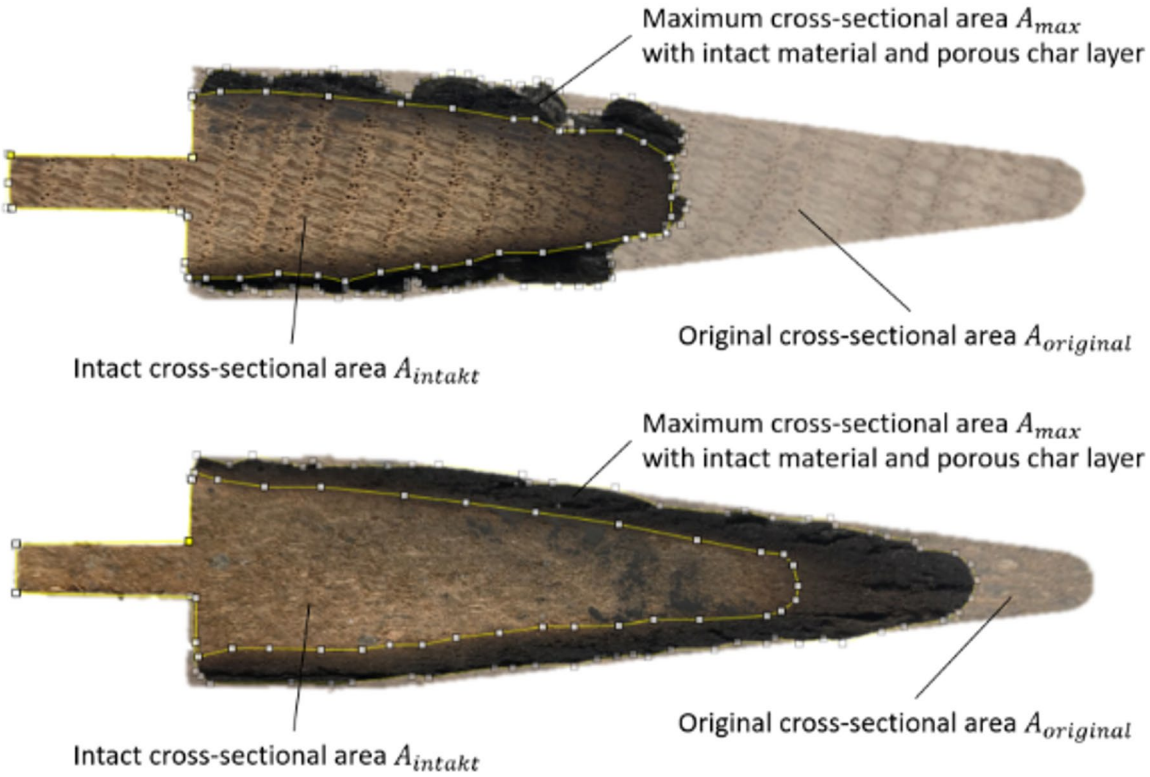


Fig. 12. Cross-sectional areas of oak (top) and TPSea-C (bottom).

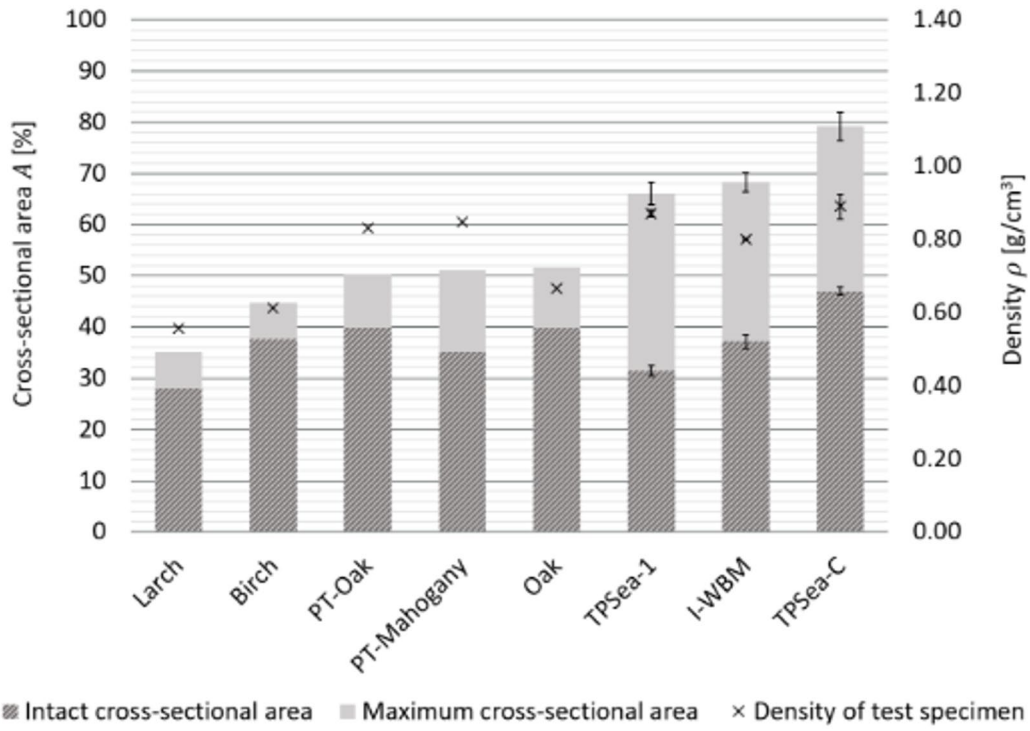


Fig. 13. Results of cross-sectional area analysis.

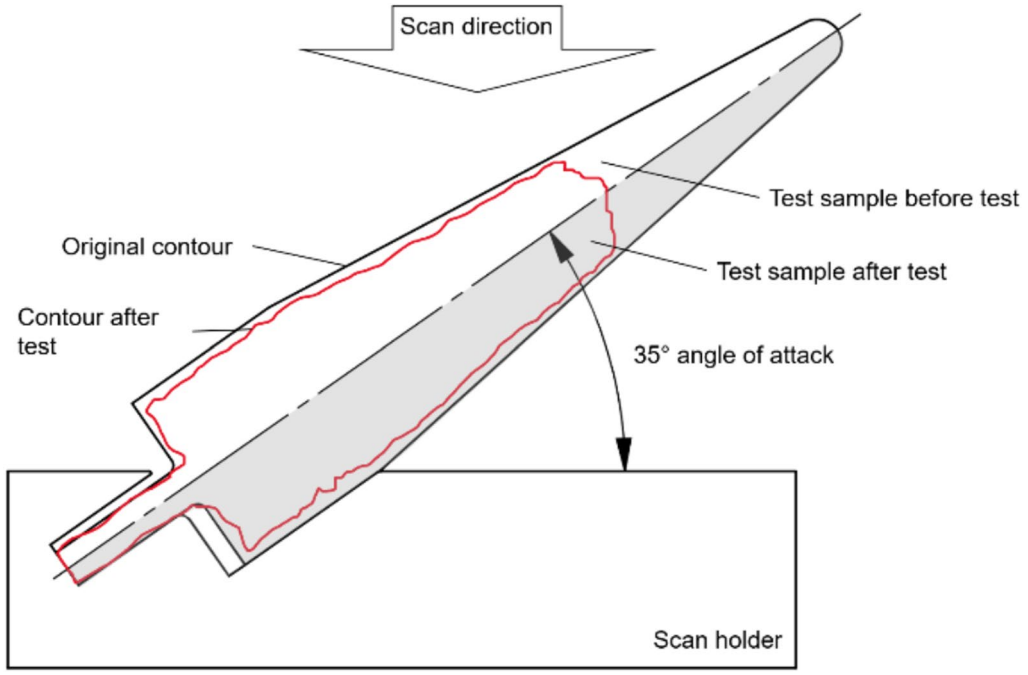


Fig. 14. Scan of the surface contour of a test specimen.

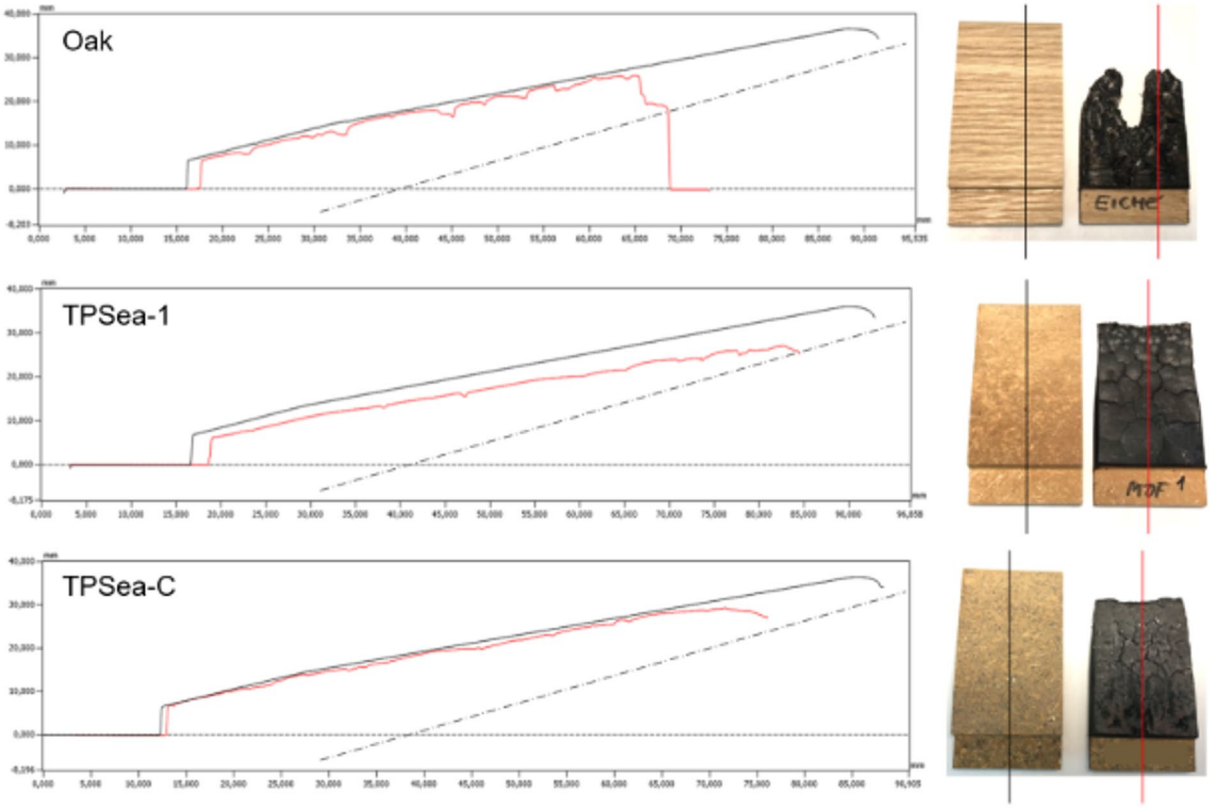


Fig. 15. Results of the surface contour of the test specimens.

formation of a cracked surface. The test specimens of the solid woods show a similar contour as the test specimen from oak. A smaller loss of material can be seen in the test specimens from TPSea-1 at the tip of the sample. Compared to the black contour line of the sample before the test, the sample has shrunk slightly in the thickness direction, as the red and black contours have a gap. The test specimen from TPSea-C show a loss of material at the tip of the sample, but the contour of the surface remains well preserved and dimensionally stable after the tests in the L2K, so that the red and black contours do not have a significant distance. Small indentations due to cracks on the surface and curvatures due to melt beads are visible in the contour.

Results and discussion

Thermogravimetric analysis (TGA) was conducted to assess the mass-loss and char-forming behaviour of the wooden (oak (*Quercus petraea, Q. robur*) and larch (*Larix decidua, Larix* spp.)) and wood-based materials (I-WBM, TPSea-0, TPSea-1 and TPSea-C). The specimens were heated from 105 to 1000 °C at a rate of 40 K/min under a nitrogen flow of 3.5 L/min. The solid woods retained the majority of their mass up to approximately 200 °C, after which a steep decrease was observed. At a temperature of 1000 °C, the residual mass was found to be 12 ± 0.006% for larch and 18 ± 0.009% for oak. TPSea-0 retained slightly more than 20 ± 0.01%, while I-WBM and TPSea-1 retained 32 ± 0.009% to 35 ± 0.01%. TPSea-C exhibited the highest residual mass, exceeding 42 ± 0.012%. The mineral deposits observed on TPSea-C after TGA are consistent with the presence of salts and mineral residues in the seagrass fibres, which may contribute to its higher residue and delayed decomposition. It is evident that the TGA results provide a screening measure of thermal decomposition and char yield within the space industry, as already described[47–49]. However, it must be noted that they do not predict performance under the transient flow and heat-transfer conditions of arc-heated wind tunnel tests like in the L2K.

The measured thermal conductivity of the wood-fibre materials ranged from 0.225 ± 0.011 W/mK for I-WBM to 0.353 ± 0.018 W/mK in-plane for TPSea-1. TPSea-C had a value of 0.252 ± 0.013 W/mK. Their specific heat capacities ranged from 1446.0 ± 173.52 J/kgK (I-WBM) and 1467.7 ± 176.12 J/kgK (TPSea-1) to 1493.2 ± 179.18 J/kgK (TPSea-C). For comparison, the reported values for CM-1 were 0.4 ± 0.1 W/mK and above 850 J/kgK, while CM-2 had values of 15 W/mK and 500 J/kgK. The wood-fibre materials therefore combine lower thermal conductivity than the reference materials with higher specific heat capacity. These properties are consistent with reduced heat transport into the fin structure and a greater amount of heat required per unit mass to increase material temperature.

The L2K tests were conducted for 120 s at a total gas mass flow of 50 g/s, a total enthalpy of 6.85 MJ/kg and a stagnation pressure of 89 hPa. The test gas was composed of 96% nitrogen and 4% air, with the fin-edge geometry specimens positioned at a distance of 120 mm from the nozzle exit. The selected condition is representative of the STORT-derived thermal load case that was utilised in the present study. At the specimen tips the measured temperature rose to a maximum of 2400 °C.

In summary, the results of the mass and cross-sectional area analysis suggest an association between material density and the thermal response of the tested wooden and wood-based materials to thermal loads. The tested wood-fibre materials showed a higher residual mass (53.2–62.0%) than solid woods (34.0–38.1%). TPSea-C had the lowest mass loss among the tested materials. In comparison, it showed up to four percentage points less mass loss than the tested mahogany specimens, despite its higher density (0.89 g/cm^3 compared with 0.85 ± 0.06 g/cm^3 for PT-Mahogany). This comparison indicates that density alone does not determine mass retention. Factors such as material composition and structure may also have a contribution. Likewise, the maximum residual cross-sectional area of the wood-fibre materials (66.1–79.2%) is higher than that of the solid woods (35.1–51.6%). It was observed that the wood-fibre samples have larger maximum residual cross-sectional areas after the test and therefore have a thicker porous carbon layer and pyrolysis zone. However, the residual intact cross-sectional ratios of the wood-fibre materials (31.5–47.0%) overlap with those of the solid woods (28.0–39.8%). All tested specimens show a loss of material at the specimen tip and a shrinkage of their geometry. A fanning of the leading edge could not be detected in the tests in the L2K. The solid woods show the biggest differences from the original contour.

Compared to the glass fibre-based CM-1, previously used by DLR, and the carbon fibre-based material PTM-1 all tested fin leading edge material variants cannot yet meet the requirements for dimensional stability and geometry retention. In particular, the test specimens of TPSea-C retain the surface contour the most and show the smallest changes in the specimen geometry as well as the lowest material loss of all tested materials. TPSea-C as a wood-fibre material showed the highest structural integrity of the porous carbon layer of all tested materials. It also has the best contour analysis results and, apart from the material loss at the specimen tip, shows good dimensional stability and surface contour. The TPSea-C material with a density of 0.89 ± 0.15 g/cm^3 could contribute to significant mass savings given the material's highly promising performance.

A thorough validation against state-of-the-art data was not possible due to the absence of a directly comparable dataset. To the authors' knowledge, no comparable assessment of solid wood and wood-fibre materials tested as fin leading edge thermal protection under comparable conditions has been published. The comparison with CM-1 and PTM-1, which were tested in the present investigation, provides an internal benchmark for assessing relative performance under the applied test conditions.

Conclusion and outlook

The results of the thermal screening and analyses after L2K tests under the selected STORT load case led to the following conclusions.

Untreated wood is not an option for a use in fin leading edges of a sounding rocket. The results show high thermal degradation and contour changes. The residual masses range from 34.0 to 38.1%, and the maximum residual cross-sectional areas range from 35.1 to 51.6%. These findings indicate that solid untreated wood is not

suitable for an application in a component of a critical primary structure assembly, as their use could potentially compromise the mission's success. In contrast, wood-fibre materials, which are characterised by higher homogeneity, additionally containing flame-retardants, seem to be promising. Compared to solid woods, they have a higher geometry and integrity retention as well as good thermal resistance and high dimensional stability. They show residual masses of 53.2–62.0% and residual maximum cross-sectional areas of 66.1–79.2%. The wood-fibre material TPSea-C performed most favourably among the tested bio-based materials in terms of material loss, contour retention and structural integrity of the porous carbon layer. It is hypothesized that, in addition to the incorporated flame-retardant additive, the seagrass fibres contribute to the flame-retardant behaviour of the material due to their naturally high salt and mineral content, thereby delaying thermal decomposition[34,35,50,51]. All wood-fibre materials have low thermal conductivities and high specific thermal capacities, which reduce the transport of heat into the fin structure. Due to their production process, there is a preferential direction of the fibres in the main plane of the board, which results in a significantly lower heat conductivity in the normal direction compared to in-plane conductivity. The measured thermal conductivities of the wood-fibre materials range from 0.225 to 0.353 W/mK, and their specific heat capacities range from 1446.0 to 1493.2 J/kgK. These properties support their potential as thermal protection materials, but do not by themselves demonstrate that the component requirements are met. The high carbon content of the materials leads to a good ablative thermal protection effect[52]. In comparison with the materials currently utilised by DLR (CM-1 and CM-2), the wood-fibre materials exhibit reduced densities and, consequently, diminished masses. Nevertheless, they are unable to satisfy the stipulated criteria for dimensional stability and geometry retention.

In summary, it can be concluded that none of the investigated bio-sourced material variants fully fulfils the requirements. However, a further material development of the wood-fibre material TPSea-C could optimise it, thus tapping into the innovation potential of sustainable spaceflight materials.

The principal outcomes of this investigation are as follows:

- Untreated solid wood showed greater thermal degradation and contour changes than the wood-fibre materials and is not considered suitable for the tested fin leading edge application in its untreated state.
- The wood-fibre materials retained more residual mass and a larger residual maximum cross-sectional area than the solid woods. The ranges of residual intact cross-sectional area overlapped, indicating that the porous residual layer should not be treated as equivalent to intact material.
- Among the tested variants, TPSea-C shows the lowest material loss and the best contour retention. Its performance is promising, but it does not yet meet all specified requirements for dimensional stability and geometry retention.
- The wood-fibre materials have lower densities than the reference materials, indicating potential for mass reduction, which can be subject to further material and structural development.
- Overall, none of the investigated bio-based material variants fully fulfils the requirements. Further development of TPSea-C may improve its performance and support the development of sustainable materials for spaceflight applications.

Detailed investigations of the mechanical material behaviour as well as the coupling of flow behaviour, dynamic structure and thermal influences can be carried out in further research. An adaptation of the geometry of the leading edge is thereby considered in order to shift the stagnation point to distribute the thermal load over a larger area. The reliability of the study's results can be improved by increasing the number of test specimens for the material screening as well as the testing in the arc-heated wind tunnel L2K. Due to the STORT flight envelope selected for this study, which represents one of the most thermally demanding high-altitude research flights for DLR MORABA, only one load case was tested, representing a limit of the study. For further investigation, tests in the arc-heated wind tunnel L2K with different pressure profiles, temperatures, gas compositions and distances between the test specimen and the nozzle outlet can be performed. Additionally, for increasing the understanding of the ablation behaviour of wood-based materials, the development of a measurement method to determine the real time ablation rate can also be taken forward. Finally, beyond material design, a focus should be placed on the analysis of the lessons learned from the active use of newly developed materials. Barriers that hinder the implementation into space system practice can play an eminent role in this analysis.

The results of this investigation can be used to open up further areas of application with less thermally stressed components like supplementary systems, tank and feed system insulation or vibration dampers. Additionally, ablative structures could be designed as "quick exchange parts" in highly stressed areas, which can be replaced quickly after each flight. Further, the results of this investigation enable the transfer of the findings to other sectors in which materials are exposed to high thermal stress as the application as an insulation and/or fire protection material in switch cabinets, vehicle construction, aviation, shipping, construction industry (especially in the housing industry and for refractory applications such as blast furnaces).

The utilisation of wood and seagrass fibre materials as substitute materials for establishing a bioeconomy in high-tech industries, such as the space industry, requires further investigation. Owing to their potentially low density, materials such as TPSea-C could contribute to mass reduction in launch vehicles and spacecraft, which may result in lower propellant requirements. Moreover, the use of renewable raw materials may reduce the dependency on non-renewable resources and offer environmental advantages over currently applied materials such as CM-1 and CM-2. Potential advantages may include a lower carbon footprint and improved biodegradability. Further in-depth evaluation and quantification of the environmental benefit can be conducted by comparing life cycle analyses according to ISO 14040:2006 of the currently applied material, e.g. CM-1 or CM-2 and its substitute material, e.g. TPSea-C.

Data availability

Please contact the corresponding author for data and materials upon reasonable requests.

Received: 12 June 2026; Accepted: 21 October 2026
Published online: 27 October 2026

References

1. Dy, D., Perrot, Y. & Pradal, R. *Micro-launchers: What is the Market? - Quick and Flexible Delivery of Small Payloads* (2017).
2. ESA. The ESA Green Agenda. https://www.esa.int/About_Us/Climate_and_Sustainability/The_ESA_Green_Agenda (2024).
3. Guenther, R., Tajmar, M. & Bach, C. Wood and wood-based materials in space applications—A literature review of use cases, challenges and potential. *Aerospace* **11**, 910 (2024).
4. Castanié, B. et al. Wood and plywood as eco-materials for sustainable mobility: A review. *Compos. Struct.* **329**, 117790 (2024).
5. Mouritz, A. P. *Introduction to Aerospace Materials* (Woodhead Publishing Limited, 2012).
6. Smithsonian Institution. De Havilland DH-98 B/TT Mk. 35 Mosquito. *Smithsonian Institution* https://www.si.edu/object/de-havilland-dh-98-btt-mk-35-mosquito%3Anasm_A19640023000.
7. Evergreen Aviation and Space Museum. The Spruce Goose - The Largest Wooden Airplane Ever Built. *Evergreen Aviation and Space Museum* https://www.evergreenmuseum.org/exhibit/the-spruce-goose/.
8. Deutsches Museum & Mosch, K. Raketenflugzeug Bachem Ba 349 'Natter'. *Deutsches Museum Digital: Raketenflugzeug Bachem Ba 349 'Natter'* https://digital.deutsches-museum.de/de/digital-catalogue/collection-object/77672/.
9. Schwarz, K. Bachem BP 20 / Ba 349 Natter: Die bemannte Rakete aus Holz. https://www.flugrevue.de/klassiker/bachem-bp-20-ba-349-natter-die-bemannte-rakete-aus-holz/ (2020).
10. Wehrmann, J. Bachem Ba 349 Natter. *Luftfahrtmuseum Hannover* https://luftfahrtmuseum-hannover.de/images/wehrmann/Bachem%20Ba%20349%20Natter.pdf (2017).
11. Smithsonian Institution. Rheintochter R I Missile. *National Air and Space Museum* https://airandspace.si.edu/collection-objects/missile-surface-air-rheinmetall-borsig-rheintochter-r-i/nasm_A19710756000 (2024).
12. Putt, D. L. German developments in the field of guided missiles. *SAE Trans.* **54**, 404–411 (1946).
13. Christopher, J. *The Race for Hitler's X-Planes - Britain's 1945 Mission to Capture Secret Luftwaffe Technology* (History Press, 2013).
14. Chertok, B. E. *Rockets and People* Vol. 1 (NASA Hist. Off., 2005).
15. Moore, J. N. *Soviet Fighters of the Second World War* (Fonthill Media, 2021).
16. Empey, D. et al. Small probe reentry investigation for TPS engineering (SPRITE). In *50th AIAA Aerospace Sciences Meeting including the New Horizons Forum and Aerospace Exposition* (American Institute of Aeronautics and Astronautics, 2012). https://doi.org/10.2514/6.2012-215.
17. SIC Human Spaceology Center. LignoSat 紹介 COMM班 – 有人宇宙学研究センター - LignoSat introduction COMM group. https://space.innovationkyoto.org/2023/08/08/lignosat_comm/ (2023).
18. Kishi, H. et al. Development of a Wooden CubeSat-LignoSat. *J. Evol. Space Act.* **2**, 218 (2024).
19. Murata, K. et al. Space exposure test of hardwood specimens in the International Space Station. *J. Wood Sci.* https://doi.org/10.1186/s10086-024-02165-x (2024).
20. WISA Plywood. The launch of WISA Woodsat is delayed due to frequency licensing | WISA PLYWOOD. *UPM Biofore Beyond Fossils* https://www.wisaplywood.com/news-and-stories/news/2021/10/the-launch-of-wisa-woodsat-is-delayed-due-to-frequency-licensing/ (2021).
21. Cooper, J. Ranger Impact Limiter. *NASA Jet Propulsion Laboratory* https://www.jpl.nasa.gov/blog/2013/11/ranger-impact-limiter (2013).
22. NASA (National Aeronautics and Space Administration). Ranger 5 - NSSDCA/COSPAR ID: 1962-055A. *NASA Space Science Data Coordinated Archive* https://nssdc.gsfc.nasa.gov/nmc/spacecraft/display.action?id=1962-055A (2021).
23. Bauer, H. E. Operational Experiences on the Saturn V S-IVB Stage. In 16 (Society of Automotive Engineers, New York, 1968). https://doi.org/10.4271/680756.
24. Bilstein, R. E. *Stages to Saturn—A Technological History of the Apollo/Saturn Launch Vehicles* (Scientific and Technocal Information Branch NASA, 1980).
25. Harvey, B. *China in Space: The Great Leap Forward* (Springer Nature, 2019).
26. Big Tech Magazine. 上得去, 回得来——中国第一颗返回式卫星诞生记 - Going up and coming back - the birth of China's first recoverable satellite. *Hainan University Science and Technology Magazine* https://baijiahao.baidu.com/s?id=1720551144331848609&wfr=spider&for=pc (2021).
27. Guenther, R. et al. First results of demonstrating the wood-fibre based thermal protection system TPSea on board Rexus 34. In (Arcachon, France, 2025).
28. Guenther, R., Tajmar, M. & Bach, C. Wood-based materials in space—An insight into the development and testing for an application on hot structures. In (Sydney, 2025). https://doi.org/10.52202/083088-0112.
29. Seibert, G. The history of sounding rockets and their contribution to European space research. In *European Space Agency*, (Special Publication) *ESA SP* 39–46 (2006).
30. Brouwer, F. et al. Advancing the resource nexus concept for research and practice. *Sustain. Nexus Forum* **31**, 41–65 (2023).
31. European Commission. Directorate General for Research and Innovation. *Categorisation System for the Circular Economy: A Sector Agnostic Categorisation System for Activities Substantially Contributing to the Circular Economy* (Publications Office, 2020).
32. Gülhan, A. et al. Selected results of the hypersonic flight experiment STORT. *Acta Astronaut.* **211**, 333–343 (2023).
33. Guenther, R., Unbehaun, H., Tajmar, M. & Bach, C. Insights on the development of the wood-fibre based thermal protection material TPSea. In (Rome, Italy, 2025). https://doi.org/10.13009/EUCASS2025-353.
34. Günther, R. E. & Unbehaun, H. WO 2024/115577 A1—Bio-based ablative thermal protection material having a mechanical function. 34 (2023).
35. Günther, R. E. & Unbehaun, H. DE 10 2022 132 031 B4 - biobasiertes ablatives thermalschutzmaterial mit mechanischer funktion. 16 (2026).
36. Niemz, P. & Sonderegger, W. Thermische Eigenschaften von Holz und Holzwerkstoffen. In *Holzphysik* 164–190 (Carl Hanser Verlag GmbH & Co. KG, 2017). https://doi.org/10.3139/9783446445468.007.
37. Institut für Arbeitsschutz der Deutschen Gesetzlichen Unfallversicherung. GESTIS-Stoffdatenbank - Natriumchlorid (NaCl). *IFA - Institut für Arbeitsschutz der Deutschen Gesetzlichen Unfallversicherung* https://gestis.dguv.de/data?name=001330 (2022).
38. Tonkonogyi, V., Ivanov, V., Trojanowska, J., Oborskyi, G. & Pavlenko, I. *Advanced Manufacturing Processes III: Selected Papers from the 3rd Grabchenko's International Conference on Advanced Manufacturing Processes (InterPartner-2021), September 7–10, 2021, Odessa, Ukraine*. (Springer Nature, 2021).
39. Niemz, P. Untersuchungen zur Wärmeleitfähigkeit ausgewählter einheimischer und fremdländischer Holzarten. *Bauphysik* **29**, 311–312 (2007).
40. DIN Deutsches Institut für Normung e.V. DIN EN ISO 10456: Baustoffe und Bauprodukte – Wärme- und feuchtetechnische Eigenschaften – Tabellierte Bemessungswerte und Verfahren zur Bestimmung der wärmeschutztechnischen Nenn- und Bemessungswerte (ISO 10456:2007 + Cor. 1:2009); Deutsche Fassung EN IS. (2010).

41. DIN Deutsches Institut für Normung e.V. DIN 68364:2003-05: Kennwerte von Holzarten (Rohdichte, Elastizitätsmodul und Festigkeiten). *Beuth Verlag GmbH* (2003).
42. Wagenführ, A. & Scholz, F. *Taschenbuch Der Holztechnik* (2018).
43. Gülhan, A., Esser, B. & Koch, U. Experimental investigation of reentry vehicle aerothermodynamic problems in arc-heated facilities. *J. Spacecr. Rockets* **38**, 199–206 (2001).
44. Gülhan, A. & Esser, B. Arc-heated facilities as a tool to study aerothermodynamic problems of reentry vehicles. In *Advanced Hypersonic Test Facilities* 375–403 (American Institute of Aeronautics and Astronautics, 2002).
45. Gülhan, A., Esser, B., Koch, U. & Hannemann, K. Mars entry simulation in the arc heated facility L2K. In 665–672 (2002).
46. Salvi, C., Hohn, O. & Gülhan, A. Characterization of ablator recession and thermal response using nonintrusive techniques. *AIAA J.* **64**, 3127–3138 (2026).
47. Helber, B., Turchi, A., Scoggins, J. B., Hubin, A. & Magin, T. E. Experimental investigation of ablation and pyrolysis processes of carbon-phenolic ablators in atmospheric entry plasmas. *Int. J. Heat Mass Transfer* **100**, 810–824 (2016).
48. Paixão, S., Peixoto, C., Reinas, M. & Carvalho, J. RETALT_TPS design and manufacturing. *CEAS Space J.* **14**, 595–604 (2022).
49. Sakraker, I., Chazot, O. & Carvalho, J. P. Performance of cork-based thermal protection material P50 exposed to air plasma: An experimental study. *CEAS Space J.* **14**, 377–393 (2022).
50. Moltó, J., Montalbán, M. G., Núñez, S. S. & Jordá, J. D. Revalorization of *Posidonia oceanica* waste for the thermochemical production of biochar. *Appl. Sci.* https://doi.org/10.3390/app12157422 (2022).
51. Anniwaer, A. et al. Steam gasification of marine biomass and its biochars for hydrogen-rich gas production. *Biomass Convers. Biorefinery* **13**, 8641–8650 (2023).
52. Meseguer, J., Pérez-Grande, I. & Sanz-Andrés, A. Spacecraft thermal control: Thermal protection systems. *Spacecraft Thermal Control* **2**, 305–325 (2012).

Acknowledgements

The authors would like to thank Prof. Dr. André Wagenführ (TUD Dresden University of Technology, Institute of Natural Materials Technology, Chair of Wood Technology and Fibre Materials Technology) for providing the laboratories and machines for material production and screening. Furthermore, the authors would like to thank Christian Zuber (German Aerospace Center (DLR), Institute for Structures and Design) for conducting thermal analysis measurements. A special thanks is reserved for the supporting engineers and mechanics at the German Aerospace Center (DLR), Supersonic and Hypersonic Technologies Department for conducting the testing at L2K.

Author contributions

All authors contributed to the study conception and design. Material preparation and TPSea material production was conducted by R.G. and H.U., data collection was conducted by R.G., H.W., O.H., O.D. and analyses were performed by R.G., O.H., H.W. and O.D. The first draft of the manuscript was written by R.G. with contributions to individual chapters from O.D. and O.H. and all authors commented, edited and reviewed on previous versions of the manuscript. M.T. and C.B. supervised the research. All authors read and approved the final manuscript.

Funding

Open Access funding enabled and organized by Projekt DEAL. Main part of this research was funded by the German Federal Ministry of Research, Technology and Space (031B1329 and 031B1486).

Declarations

Competing interests

The authors have no relevant interests, both financial and non-financial, to disclose.

Additional information

Correspondence and requests for materials should be addressed to R.G.

Reprints and permissions information is available at www.nature.com/reprints.

Publisher's note Springer Nature remains neutral with regard to jurisdictional claims in published maps and institutional affiliations.

Open Access This article is licensed under a Creative Commons Attribution 4.0 International License, which permits use, sharing, adaptation, distribution and reproduction in any medium or format, as long as you give appropriate credit to the original author(s) and the source, provide a link to the Creative Commons licence, and indicate if changes were made. The images or other third party material in this article are included in the article's Creative Commons licence, unless indicated otherwise in a credit line to the material. If material is not included in the article's Creative Commons licence and your intended use is not permitted by statutory regulation or exceeds the permitted use, you will need to obtain permission directly from the copyright holder. To view a copy of this licence, visit http://creativecommons.org/licenses/by/4.0/.

© The Author(s) 2026